Solvent effects on isolated formamide and its monohydrated complex: observations from PCM study†

Anqun Chen,[a] Xuemei Pu,*[ab] Shuhua He,[a] Yanzhi Guo,[a] Zhining Wen,[a] Menglong Li,[a] Ning-Bew Wong[c] and Anmin Tian[a]

Received (in Montpellier, France) 3rd February 2009, Accepted 31st March 2009
First published as an Advance Article on the web 18th May 2009
DOI: 10.1039/b902149c

A polarizable continuum model (PCM), at the B3LYP/6-311++G (d,p) level of theory, is used to study solvent effects on isolated formamide and its monohydrated complex. Six varying kinds of solvent (*viz*. water, dimethyl sulfoxide, acetonitrile, ethanol, tetrahydrofuran, carbontetrachloride) are selected to model different polarity environments. The roles of non-specific solvation and specific H-bonding associated with the bound water in influencing geometries, vibrational frequencies, binding energies, ^{1}H chemical shifts and n → π* transition energies are discussed for formamide. Natural bond orbital (NBO) and atoms in molecules (AIM) theories are used to analyze the nature of H-bonding and the origin of solvent effects. Significant red- and blue-shifts are observed for the frequencies of formamide upon solvation and formation of hydrogen bonds, respectively. Both the solvation and the H-bonding increase the ^{1}H chemical shifts of amino protons and the n → π* transition energy, while the chemical shift of formyl proton is nearly insensitive to the two effects. The role of the specific H-bonding in influencing molecular properties is lessened by the solvation since the solvent lowers the binding energy of the complex, while the solvent effect is also modulated by the H-bonding through a specific intermolecular interaction. Compared with non-polar solvents, polar solvents have a more obvious effect on the properties examined. Furthermore, all the variations show a large dependency on the dielectric constant up to a value of ~10, after which no further changes are observed.

1. Introduction

Formamide (FA) is the simplest molecule containing an amide linkage (–CO–NH–). Its solvated complex has been the subject of intense interests from experimental and theoretical researches owing to implication for protein hydration.[1–36] Geometries, H-bond interaction, spectroscopic properties (such as electronic, vibrational, rotational and NMR spectra), tautomerism and hydrolysis have been studied for FA·$(H_2O)_n$ (n = 0–4) systems in vacuum, liquid and solvents.[5–36] In these researches, solvent effects generally focus on aqueous environment while other organic media were seldom considered. Electronic spectra of formamide in acetonitrile[26,27] and cyclohexane solutions[27,29] were investigated by some experiments. Later, Hirst[27] used an *ab initio* method to study the electronic spectrum of formamide in cyclohexane. Taha *et al.*[16] determined experimental internal rotation barriers for formamide monomer in three solutions (water, dimethyl sulfoxide, acetonitrile) and calculated the barrier in a series of dielectric constants ranging from 1 to 109 using self-consistent isodensity polarizable continuum model (SCIPCM) at the HF/6-311++G** level of theory. Recently, Zhou[5] studied binding energies of 1 : 1 complexes of formamide with water using the Onsager reaction field model with a range of dielectric constants from 2 to 80 at B3LYP/6-311++(d,p) level and drew a conclusion that solvent generally increases the binding energies, opposite to results from some similar researches.[14,15,37]

The focus of this paper is the effect of organic solvents with different polarity on the interaction between formamide and water. The interests mainly stem from the use of enzymes in organic media with low water content, which has been one of the most exciting facets of enzymology in recent times since enzymatic reactions in nonaqueous solvents provide numerous synthetic and processing advantages.[38,39] However, native enzymes almost universally exhibit low activities in organic solvents.[40,41] Factors which contribute to this activity drop are complicated. Water stripping has been considered as one main reason.[39,42] In nonaqueous media, a low water presence is still

[a] *Faculty of Chemistry, Sichuan University, Chengdu, 610064, People's Republic of China. E-mail: xmpuscu@scu.edu.cn; Fax: +86-028-85412800*
[b] *State Key Laboratory of Biotherapy, Sichuan University, Chengdu, 610064, People's Republic of China*
[c] *Department of Biology and Chemistry, City University of Hong Kong, Kowloon, Hong Kong*

† Electronic supplementary information (ESI) available: Table S1: Geometrical parameters (bond lengths and bond angles) and vibrational stretching frequencies for formamide in the isolated form and in the complexed form in the gas phase and in six solvents calculated at B3LYP/6-311++G(d,p) level of theory and some corresponding experimental values. Table S2: GIAO B3LYP/aug-cc-pVTZ calculated ^{1}H NMR chemical shifts and variations of H chemical shifts upon solvation and complexation in the gas phase and in six selected solvents within the framework of the IEF-PCM model. Fig. S1: Dependences of variations in n → π* transition energies of formamide upon solvation on dielectric constants of solvents in the monomer and the complex. See DOI: 10.1039/b902149c

required for catalysis of enzymes,[43,44] and the control of water is exerted by the amount of molecules bound to the enzyme rather than its level in the organic solvent.[45] It is found that the polar solvent shows higher ability than a nonpolar one to remove (or strip) bound water from protein[46] and a dependence of activity on the polarity of the solvent was found for some enzymes,[40a,b] dropping as the polarity is increased. However, experimental data for understanding the nature of effects of nonaqueous solvents on interactions between the enzyme and the bound water are limited due to the complexity of the protein structure and the molecular nature of the issue. As well-known, progress of computational quantum chemistry has offered alternative approaches to obtain microscopic information at the molecular level and supplement experimental investigations. The size of enzyme, however, limits high levels of quantum chemical calculation, which can provide a reliable physical background. Therefore, we, herein, select one monohydrated formamide, where water is simultaneously acting as a proton donor to the carbonyl group oxygen atom and as a proton acceptor from the amino group, as a prototype of bound water and protein in organic media with low water content (see Fig. 1). The cyclic formamide–water complex has been identified as the most stable small cluster in previous microwave,[2,3] infrared[4] studies and some theoretical studies.[1,5,6] Effects of solvent polarity on the conformer are studied using the polarizable continuum model (PCM).[47] In the PCM, the solvent is represented as a homogeneous dielectric continuum where a solute is placed in a molecule-shaped cavity, neglecting any reference to the atomistic nature of the solvent. Thereby, the solvent effect derived from the PCM model indicates non-specific electrostatic effects, not considering any specific solute–solvent interactions. However, the PCM accounts already for large parts of the solvent effect, as demonstrated on many occasions to be quite successful in investigating molecular properties in solution.[12,48–53] To model different media environments, six solvents of varying nature are selected, spanning from nonpolar (carbon tetrachloride, CCl_4: $\varepsilon = 2.23$), weakly polar (tetrahydrofuran, THF, $\varepsilon = 7.58$), polar (ethanol, ETH, $\varepsilon = 24.55$; acetonitrile, ACN, $\varepsilon = 36.64$; dimethyl sulfoxide, DMSO, $\varepsilon = 46.70$), to highly polar (water, WAT, $\varepsilon = 78.39$). On the other hand, effects of the selected solvents on formamide monomer are studied in the present work. The observations obtained from the two prototypes (*viz*. the isolated formamide monomer and its complex) in the gas phase and in six different-polarity solutions enables (1) to gain insight into the role of non-specific solvation in influencing geometries, vibrational frequencies, binding energies, ^{1}H chemical shifts and $n \rightarrow \pi^*$ transition energies of formamide by comparisons of results from the solutions with those from the gas phase; (2) to obtain information with respect to the role of the specific hydrogen bonding between the solute and the bound water in modulating the solvent effects, by means of analyzing differences in the molecular properties between the monomer and its monohydrated complex. (3) to probe, at least for the present system, the physical origin of solvent effects and the nature of hydrogen bonding with the aid of natural bond orbital (NBO) and atoms in molecules (AIM) analyses. Herein, we are concerned less on the absolute value of the calculated property, but more so on its changes induced by solvation and H-bonding, since our purpose is to provide helpful information, by employing the model system, for better understanding the interaction between the bound water and enzyme in organic media with different polarities.

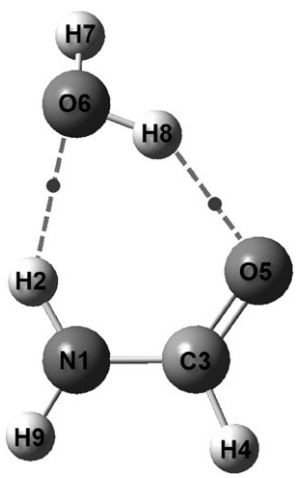

Fig. 1 Geometry of monohydrated complex (**II**) calculated at the B3LYP/6-311++G(d,p) level of theory (the two dots indicate the bond critical points.)

2 Computational methods

The continuum solvation model adopted here is the so-called integral equation formalism, *viz*. IEF-PCM.[54] For all species under study, B3LYP geometry optimization has been performed at the 6-311++G(d,p) level in gas-phase and the six kinds of solvents within the framework of the IEF-PCM model. All the geometries are confirmed as stationary structure by the presence of only real frequencies at the same level of theory. The frequency values have been scaled by a factor of 0.963.[9]

Binding energies have been calculated taking into account basis set superposition error (BSSE). BSSE is obtained by reoptimizing the structure of the complex in the gas-phase at the B3LYP/6-311++G(d,p) level using the counterpoise (CP) method[55] and is assumed to be equal in gas-phase and with PCM.[37]

The topological properties of electron charge densities are calculated by atoms in molecules (AIM)[56] method using AIM2000 software[57] at B3LYP/6-311++G(d,p) wave function. The orbital interactions of all the optimized structures are further analyzed using natural bond orbital (NBO) theory of Weinhold and co-workers[58] at the B3LYP/ 6-311++G(d,p) level.

Calculations of NMR chemical shielding constants are performed using the "gauge-including atomic orbital" (GIAO) method.[59,60] Several DFT functionals, *viz*. B3LYP, OPBE, OPW91 and KT3, are evaluated in gas-phase calculation for ^{1}H chemical shifts. The Dalton Quantum Chemistry Program[61] is employed to carry out the KT3 calculation. The ^{1}H chemical shift is a difference of isotropic shielding constants of the studied system with respect to the tetramethylsilane (TMS) reference molecule. The structures of

TMS, as a standard, are optimized in the gas phase and the six selected solvents at the B3LYP/6-311++G(d,p) level. To be comparable, the calculation of the nuclear shielding of the reference compound and the isolated formamide as well as the monohydrated one are carried out at the same level of theory.

The lowest dipole allowed n → π* vertical excitation energies of all optimized species are calculated at the B3LYP/6-311++G(d,p) level, using time-dependent density function theory (TDDFT).[62] The IEF-PCM model is introduced in NBO, GIAO and TDDFT calculations for all the "solvated" systems studied here so as to include solvent effects.[12,48–51] All the calculations except for AIM and KT3 are performed using the Gaussian03[63] series of programs.

3. Results and discussion

Fig. 1 shows the structure of the monohydrated complex ($NH_2CHO\cdots H_2O$). Calculated geometrical parameters and vibrational stretching frequencies for isolated formamide and its monohydrated complex in the gas phase and the six kinds of solvents are presented in Table S1 in ESI,† along with some available experimental values.[2,10–12] Variations of the bond lengths and the frequencies upon solvation and complexation are given in Table 1. The topological parameters of the H···O contacts derived from the AIM calculation, the H-bond distances and the binding energies with inclusion of counterpoise correction for BSSE in different media environments are summarized in Table 2. Second-order perturbation energies derived from the NBO calculation are contained in Table 3. The ^{1}H chemical shifts of formamide are collected in Table S2 in ESI.† Table 4 lists the n → π* vertical transition energies of formamide. All values associated with dielectric constants of solvents (ε) include the result from gas phase (ε = 1.00).[64]

3.1 Geometries and vibrational analysis

There are some experimental studies on some structure parameters of isolated formamide in gas phase (see Table S1 in ESI†).[2,10] By comparing the calculated with the experimental values, close agreement is obtained. In addition, data in Table 1 clearly show that the structural data in the solvents does not deviate much from the gas-phase data, either for the complexed form or the isolated molecule. Formamide remains planar and its bond angles are nearly unchanged on passing from the gas phase to the solution environment (see Table S1 in ESI†). The bond length of formamide, however, displays some minor to moderate variations upon solvation. As seen from Fig. 2, the solvent effect on the bond length of formamide in the isolated monomer form is similar to the complexed form with the exception of the proton donating N1–H2 bond. When passing from gas phase to the solution, for both the monomer and the complex, the N1–H9 and C3═O5 bonds are elongated while the C3–H4 and C3–N1 bonds are shortened. Interestingly, the solvent displays an opposite effect on the proton donating N1–H2 bond of the monomer to that of the complex. The solvent induces an elongation of the N1–H2 bond in the monomer but leads to shortening in the hydrated complex (see Table 1 and Fig. 2), implying the effect of the bound water molecule. As shown in Fig. 2, the non-specific

Table 1 Variations on bond lengths (in Å) and vibrational stretching frequencies[a] (cm^{-1}) of formamide upon solvation and complexation in the monomer (**I**) and in its monohydrated complex (**II**), calculated at B3LYP/6-311++G(d,p) level of theory[b]

	GAS	CCl_4			THF			ETH			ACN			DMSO			WAT		
		sol − gas			sol − gas			sol − gas			sol − gas			sol − gas			sol − gas		
	II − **I**	**I**	**II**	**II** − **I**	**I**	**II**	**II** − **I**	**I**	**II**	**II** − **I**	**I**	**II**	**II** − **I**	**I**	**II**	**II** − **I**	**I**	**II**	**II** − **I**
ΔR_{N1-H2}	0.007	0.001	0.000	0.006	0.003	−0.001	0.003	0.004	−0.001	0.002	0.004	−0.001	0.002	0.004	−0.001	0.002	0.004	−0.001	0.002
ΔR_{N1-H9}	−0.001	0.002	0.002	−0.001	0.004	0.005	0.000	0.005	0.006	0.000	0.005	0.006	0.000	0.005	0.006	0.000	0.005	0.006	0.000
ΔR_{C3-H4}	−0.003	−0.001	−0.001	−0.003	−0.002	−0.002	−0.003	−0.002	−0.002	−0.003	−0.002	−0.002	−0.003	−0.002	−0.002	−0.003	−0.003	−0.002	−0.002
$\Delta R_{C3=O5}$	0.011	0.006	0.005	0.01	0.011	0.009	0.009	0.014	0.011	0.008	0.014	0.011	0.008	0.014	0.011	0.008	0.015	0.011	0.007
ΔR_{C3-N1}	−0.012	−0.007	−0.003	−0.008	−0.013	−0.007	−0.006	−0.015	−0.009	−0.006	−0.016	−0.009	−0.005	−0.016	−0.009	−0.005	−0.016	−0.009	−0.005
$\Delta\nu_{asN1-H2}$	−23.7	−33.3	−29.4	−19.8	−71.8	−59.5	−11.4	−86.5	−70.7	−7.9	−89.1	−72.9	−7.5	−90.0	−73.7	−7.4	−91.7	−75.6	−7.6
$\Delta\nu_{sN1-H2}$	−96.9	−29.2	1.1	−66.6	−62.8	2.1	−32	−74.8	1.3	−20.8	−77.1	1.0	−18.8	−77.9	0.8	−18.2	−79.4	−0.2	−17.7
$\Delta\nu_{C3-H4}$	35.3	13.7	8.9	30.5	22.8	15.6	28.1	25.8	18.1	27.6	26.3	18.1	27.1	26.2	18.2	27.3	26.9	18.6	27
$\Delta\nu_{C3=O5}$	−30.0	−36.3	−26.0	−19.7	−68.0	−50.6	−12.6	−80.7	−60.5	−9.8	−82.6	−61.8	−9.2	−83.6	−62.4	−8.8	−85.8	−64.2	−8.4
$\Delta\nu_{C3-N1}$	49.0	8.9	0.7	40.8	17.6	0.9	32.3	20.6	1.1	29.5	21.1	0.9	28.8	21.5	1.0	28.5	21.6	0.6	28.1

[a] Frequencies scaled by 0.963.[9] [b] **II** − **I** denotes subtracting the data of the monomer from that of the corresponding complex, which may characterize effects of the specific H-bonding; sol − gas denotes subtracting the data in the gas-phase from that in solvent, which may characterize effects of non-specific solvation. **I** denotes the monomer; **II** denotes the complex.

Table 2 H-Bond distances ($r_{O\cdots H}$, in Å) and electron densities (ρ, in a.u.) and Laplacian values ($\nabla^2\rho$, in a.u.) at bond critical points of H-bonds and two types of binding energies derived from total electronic energies (ΔE, in kcal mol^{-1}) and Gibbs free energies (ΔG, in kcal mol^{-1}) with the inclusion of counterpoise correction for BSSE for the complex in gas phase and in the six solutions[a]

Solvent	H-bond	ρ	$\nabla^2\rho$	$r_{O\cdots H}$	ΔE	ΔG
GAS	O6···H2	0.0193	0.0752	2.058	-8.86	1.96
	O5···H8	0.0274	0.0936	1.921		
CCl_4	O6···H2	0.0181	0.0689	2.096	−6.21	4.52
	O5···H8	0.0276	0.0936	1.917		
THF	O6···H2	0.0165	0.0609	2.150	−3.92	6.66
	O5···H8	0.0283	0.0953	1.907		
ETH	O6···H2	0.0156	0.0565	2.183	−3.11	7.35
	O5···H8	0.0289	0.0970	1.897		
ACN	O6···H2	0.0154	0.0556	2.190	−2.99	7.46
	O5···H8	0.0290	0.0972	1.896		
DMSO	O6···H2	0.0154	0.0557	2.190	−2.92	7.54
	O5···H8	0.0291	0.0973	1.895		
WAT	O6···H2	0.0151	0.0544	2.200	−2.88	7.52
	O5···H8	0.0291	0.0974	1.895		

[a] ΔE = E(in complex) − E(in monomer); ΔG = G (in complex) − G(in monomer).

Table 3 Second-order perturbation energies ($E^{(2)}$, in kcal mol^{-1}) associated with the hydrogen bonding between formamide and the bound water, derived from NBO calculations at the B3LYP/6-311++G(d,p) theory level

Solvent	$E^{(2)}(n_{O6} \rightarrow \sigma^*_{N1-H2})$	$E^{(2)}(n_{O5} \rightarrow \sigma^*_{O6-H8})$
GAS	4.61	6.92
CCl_4	4.24	7.26
THF	3.65	7.79
ETH	3.31	8.15
ACN	3.24	8.21
DMSO	3.25	8.24
WAT	3.13	8.25

Table 4 ^{1}H NMR isotropic shielding constants and chemical shifts[a] (in parentheses) of isolated formamide in the gas phase (B3LYP/6-311++G(d,p) optimized geometry), calculated using four functionals of DFT and 6-311++G(d,p) basis set[b]

Nucleus	OPBE	OPW91	KT3	B3LYP
H2	27.18 (4.53)	27.20 (4.52)	27.42 (4.49)	27.36 (4.61)
H4	23.32 (8.39)	23.34 (8.38)	23.63 (8.28)	23.60 (8.37)
H9	27.17 (4.54)	27.20 (4.52)	27.54 (4.37)	27.50 (4.47)

[a] Chemical shifts of hydrogen nuclei are referred to TMS. [b] Results are in units of ppm.

solvation shift in the bond length, *viz*. ΔR(sol − gas) = R(in a given solution) − R(in a gas phase), including the elongation and the contraction, show large dependency on the dielectric constant up to a value of ~10, after which no further changes are observed.

Comparisons of the data in the monomer (**I**) and in the complex (**II**) show that the N1–H9 and the C3–H4 bond lengths are almost insensitive to addition of the water molecule, as depicted in Fig. 3. Upon complexation, the proton donating N1–H2 bond and the proton accepting C3═O5 bond are elongated while the C3–N1 bond is shortened (see Table 1 and Fig. 3). Similarly, the bond length variation upon complexation, *viz*. ΔR(**II** − **I**) = R(in complex) − R(in monomer), is found to be largest in the gas-phase and second largest in the nonpolar solvent (carbon tetrachloride). As solvent polarity increases up to a relatively high level ($\varepsilon > 10$), the difference in the ΔR(**II** − **I**) values among polar solvents disappears (see Fig. 3). In other words, non-specific solvation would weaken the bond length shift upon association with the bound water molecule, especially polar solvation. However, the extent of weakening is not further amplified by the solvent polarity when the dielectric constant of the environment is higher than a value of ~10.

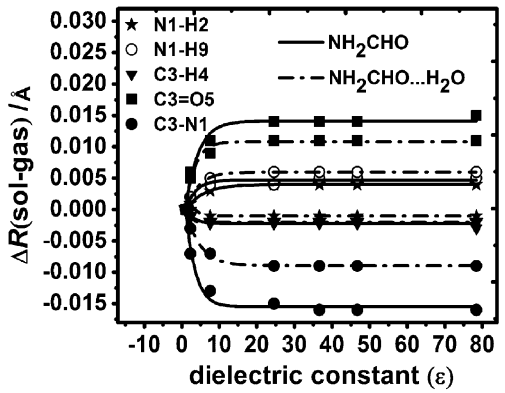

Fig. 2 Dependences of solvent-induced shifts in bond lengths of formamide (ΔR(sol − gas)) on dielectric constants of solvents (ε) in the isolated form (—) and the complexed form (---).

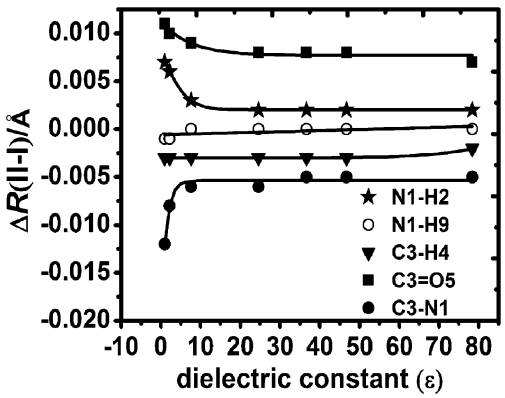

Fig. 3 Dependences of bond length variations of formamide owing to complexation (ΔR(**II** − **I**)) on dielectric constants of solvents (ε).

On the other hand, red shifts in the stretching vibrational frequencies of the proton donating N1–H2 bond and the C3═O5 bond are observed for formamide monomer owing to solvation. In the monomer, the computed gas-to-solution red-shifts, *viz*. $\Delta\nu$(sol − gas) = ν(in a given solution) − ν(in gas phase), are in the ranges of 33–92 cm^{-1} for the N–H asymmetric stretching vibration frequencies ($\Delta\nu_{asN-H}$(sol − gas)), 29–79 cm^{-1} for the N–H symmetric stretching frequencies ($\Delta\nu_{sN-H}$(sol − gas)) and 36–86 cm^{-1} for the C3═O5 frequencies ($\Delta\nu_{C3=O5}$(sol − gas)), as shown in Table 1 and Fig. 4. In contrast, the solvent causes blue-shifts of 13–27 and 8 ~ 22 cm^{-1} for the ν_{C3-H4} and the ν_{C3-N1} in the monomer, respectively. The gas-to-solution shifts in the frequencies ($\Delta\nu$(sol − gas)) also show a positive dependency on the dielectric constant (ε) of the environment, increasing with

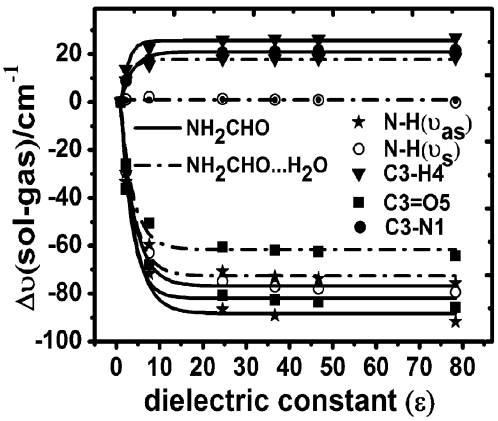

Fig. 4 Dependences of solvent-induced shifts in vibrational stretching frequencies of formamide ($\Delta\nu$(sol − gas)) on dielectric constants of solvents (ε) in the monomer (—) and its monohydrated complex (---).

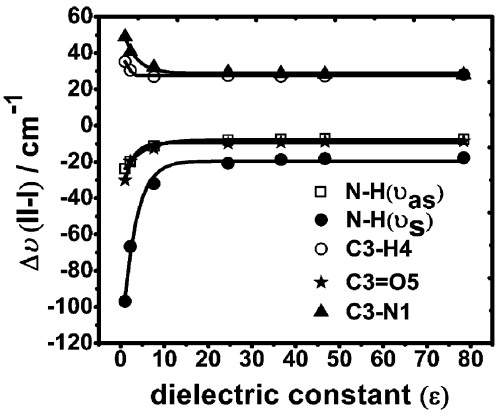

Fig. 5 Dependences of shifts in vibrational stretching frequencies of formamide due to complexation ($\Delta\nu$(**II** − **I**) on dielectric constants of solvents (ε).

increasing solvent polarity. Some experimental researches[10–12] on formamide (see Table S1 in ESI†) reported that the red shifts are 37 cm^{-1} for the ν_{N-H} in carbon tetrachloride solution, 99 cm^{-1} for the $\nu_{as\ N-H}$ and 91 cm^{-1} for the $\nu_{s\ N-H}$ in acetonitrile solution, compared with the corresponding values of 33, 89 and 77 cm^{-1} derived from our calculations for the monomer. Similar to the variation in the bond length, the solvation shifts in the calculated frequencies (see Fig. 4) exhibit a sharp decrease with an increase in the dielectric constants (ε) of solvents in the relatively low ε region ($\varepsilon < 10$). In contrast, in the higher-ε region, the frequency shift upon solvation is rather insensitive to the solvent polarity. The dependence of C═O frequency of formamide on the solvent dielectric constant shown in Fig. 4 is similar to experimental observations on the dependence of C═O frequency of formaldehyde on solvents (cyclohexane, chloroform, THF, ACN, DMSO and water) reported by Begue,[65] who showed that the variation of $\nu_{C=O}$ is in a rather narrow range (less than 5 cm^{-1}) on going from THF to ACN to DMSO to water, thus confirming the reliability of computational model selected in the present work.

As for the complex, the frequency variations induced by the solvents ($\Delta\nu$(sol − gas)) are similar to those in the monomer with the exception of the $\nu_{s\ N-H}$ and ν_{C3-N1} (see Fig. 4). The red shifts owing to solvation still be observed for the $\nu_{as\ N-H}$ and the $\nu_{C3=O5}$ while the $\Delta\nu_{C3-H4}$(sol − gas) are blue-shifted. However, the shift in the complex is smaller than that in the corresponding monomer. Interestingly, the gas-to-solution shifts in the $\nu_{s\ N-H}$ and ν_{C3-N1} significantly differ from those in the monomer, being almost insensitive to the solvent polarity, thereby indicating remarkable role of the specific interaction between the bound water and formamide in the solvent effects.

Compared the frequencies in the monomer with those in the corresponding complex, significant red-shifts ($\Delta\nu$(**II** − **I**) upon formation of H-bonds are observed for the ν_{N-H} and the $\nu_{C3=O5}$ while blue-shifts are found for the ν_{C3-N1} and ν_{C3-H4} (Fig. 5). Furthermore, the frequency shifts ($\Delta\nu$(**II** − **I**)) induced by the complexation, either blue or red shift, are significantly weakened by the solvation, decreasing with increasing polarity of solvents. Similarly, the extent of weakening nearly converges to a constant value in the case of $\varepsilon > 10$, as illustrated in Fig. 5.

3.2 AIM and NBO analysis

To gain more insight into the solvent effects on the interaction between formamide and the bound water, the electron density topological analysis based on the AIM theory is carried out for all the monomers and the complexes studied here. Popelier and Koch[66,67] proposed some topological criteria based on the AIM theory[66,68] to detect and characterize hydrogen bonding. The most prominent evidence of hydrogen bonding is: (i) correct topological pattern (*i.e.*, the existence of a bond critical point (BCP) and a bond path); (ii) proper value of electron density and Laplacian of electron density at this BCP. These topologic properties calculated using the AIM2000 program are listed in Table 2.

In terms of the AIM calculation results, two bond critical points (BCPs) in the contact of formamide and the water molecule are found for the complex in the gas phase and the six solvents. One bond path of the two BCPs links the oxygen atom of the water molecule and one amino hydrogen of formamide and the other links the oxygen atom of the carbonyl group of formamide and one hydrogen of the water molecule, as visualized in Fig. 1. When passing from the gas phase to the six solutions, the corresponding Laplacian values of electron densities at the BCPs ($\nabla^2\rho$) vary within 0.0544–0.0974 a.u. and electron densities at the BCPs (ρ) range between 0.0151 and 0.0291 a.u., much smaller than that of a covalent bond. These results clearly indicate that the N1–H2···O6 and O6–H8···O5 contacts are classical hydrogen bonds ($\rho \approx 10^{-2}$ and positive $\nabla^2\rho$).[69,70] Compared with the gas phase, the solvents decrease the electron density (ρ) at the BCP of N1–H2···O6 hydrogen bond but increase the ρ value at the BCP of the O6–H8···O5 hydrogen bond (see Table 2). As a result, the H2···O6 distance is elongated while the H8···O5 distance is shortened by the solvents, as confirmed by a good correlation between the ρ value and the H-bond distance (see eqn (1)).

$$r_{O\cdots H} = 2.502 - 21.07\rho_{O\cdots H};\ R = -0.994 \qquad (1)$$

The observations imply that the solvents enhance the H-bonding of the O6–H8···O5 contact but weaken the N1–H2···O6 contact, especially polar solvents.

To further understand the nature of solvent effects on the hydrogen bond interaction, NBO analysis in the gas phase and solutions have been carried out at the B3LYP/6-311++G(d,p) theory level, based on the optimized structures at the same level. The second-order perturbation energies derived from the NBO calculation are presented in Table 3. The NBO analysis reveals that the lone pair of the oxygen atom of the water molecule (n_{O6}) interacts with the σ antibonding orbital of the proton donating N1–H2 bond (σ^*_{N1-H2}) of formamide (FMA) and the lone pair of oxygen atom of the carbonyl group (n_{O5}) of formamide (FMA) interacts with the σ antibonding orbital of the proton donating O6–H8 bond of the water molecule (σ^*_{O6-H8}) in the gas-phase and solvated systems. The observation further confirms the two H-bonds between the solute and the water molecule. When going from gas phase to the solutions, the second-order perturbation energies $E^{(2)}$ associated with these interactions range from 4.61 to 3.13 kcal mol^{-1} for $n_{O6}(H_2O) \rightarrow \sigma^*_{N1-H2}$(FMA) and from 6.92 to 8.25 kcal mol^{-1} for n_{O5}(FMA) $\rightarrow \sigma^*_{O6-H8}(H_2O)$. Compared with gas-phase, the solvents increase the $E^{(2)}(n_{O5}(FMA) \rightarrow \sigma^*_{O6-H8}(H_2O))$ values but lowers the $E^{(2)}(n_{O6}(H_2O) \rightarrow \sigma^*_{N1-H2}(FMA))$. The result suggests that the solvent weakens the H-bond interaction associated with $n_{O6}(H_2O) \rightarrow \sigma^*_{N1-H2}$(FMA) but enhances the H-bonding of $n_{O5}(FMA) \rightarrow \sigma^*_{O6-H8}(H_2O)$, in agreement with the AIM analysis above. The $E^{(2)}$ value correlates well with the electron densities in the H-bond critical points ($\rho_{O\cdots H}$), as shown in eqn (2).

$$E^{(2)} = -2.195 + 352.41\rho_{O\cdots H};\ R = 0.996 \qquad (2)$$

The correlations presented in eqn (1) and (2) indicate that the solvent induces variation of the electron density in the intermolecular H-bonds (*viz.* $\rho_{O\cdots H}$) by means of influencing the intermolecular interaction associated with the $n_{O6}(H_2O) \rightarrow \sigma^*_{N1-H2}$(FMA) and $n_{O5}(FMA) \rightarrow \sigma^*_{O6-H8}(H_2O)$. As a result, the hydrogen bond distances are changed.

3.3 Binding energies of the complex

Binding energies of complexes can yield direct estimation of intermolecular interactions measured at the molecular scale. Thereby, it would provide more direct information about solvent effects on the interaction strength between the solute and the water molecule. Table 2 lists two kinds of binding energies obtained in terms of differences in electronic energies and Gibbs free energies between the complex and the monomer, respectively. As can be seen from Table 2, the absolute values in the two classes of binding energies are significantly different. However, the variation trends presented by them are similar, both suggesting that the binding strength is highest in the gas phase while the solvent weakens the interaction strength, especially in polar solvents. Similarly, the differences in the binding strength between different-polarity environments gradually diminish with increasing dielectric constant of the solvent. The solvent effect on the binding energy in the present work differ from observations from Zhou[5] which reported that the binding energies of 1 : 1 complexes of formamide with water increase with increasing the solvent polarity, but consistent with findings from other groups.[14,15,37] Sneddon[14] reported that the amide hydrogen bond is more stable in CCl_4 than in water. Results from the formamidine–formic acid complex also revealed that the H-bond strength is reduced rapidly with increasing dielectric constant.[15] Recently, Mennucci[37] reported that solvents decrease binding energies of dimers, trimers and tetramers in studying the structure of acetonitrile, formamide and their mixtures in the liquid state.

Good linear correlations are observed between the binding strength and the sum of two H-bond distances and the sum of their electron densities, as shown in eqn (3)–(6).

$$\Delta E = 212.98 - 51.42\sum r_{O\cdots H};\ R = -0.987 \qquad (3)$$

$$\Delta E = -109.01 + 252\,215\sum \rho_{O\cdots H};\ R = 0.995 \qquad (4)$$

$$\Delta G = -187.7 + 47.79\sum r_{O\cdots H};\ R = 0.985 \qquad (5)$$

$$\Delta G = 111.79 - 2349.10\sum \rho_{O\cdots H};\ R = -0.994 \qquad (6)$$

In terms of the series of correlations suggested by eqn (1)–(6), we can explain the origin of non-specific solvent effects on the binding strength between formamide and the bound water. The solvent polarity first changes the intermolecular interaction associated with the $n_{O6}(H_2O) \rightarrow \sigma^*_{N1-H2}$(FMA) and $n_{O5}(FMA) \rightarrow \sigma^*_{O6-H8}(H_2O)$, and then causes a decrease in the total electron density in the BCPs of the two H-bonds and accordingly increases the total distances of the two H-bonds. Ultimately, the interaction of formamide and the bound water molecule is weakened, as reflected by smaller ΔE and larger ΔG. From these observations we can assume that the fact that a polar solvent has a higher ability to remove protein-bound water than non-polar solvent[46,71] is partly attributed to its marked role in weakening the H-bonds between the protein and water.

3.4 NMR chemical shifts of hydrogen nucleus

The relationships between protein structure and NMR chemical shifts have been studied extensively by experiments and theories because NMR chemical shift predictions can significantly aid protein structure and refinement.[72–75] Since the hydrogen nucleus is the most sensitive to environment, solvent effects on hydrogen nuclear magnetic shielding parameters have been the subject of experimental and theoretical researches.[16,17,19,48,49,76,77] Herein, we also discuss effects of the non-specific solvation and the specific H-bonding between the solute and the water molecule on the ^{1}H chemical shift of formamide, aiming at supplementing experimental NMR studies in non-aqueous enzymology.

3.4.1 Method analysis. For accurate calculations of chemical shifts, an appropriate computational method and a basis set should be chosen. During the last few decades, a number of methods have been developed for calculations of the NMR chemical shielding, and it is commonly accepted that accurate prediction of these properties requires taking into account electron correlation effects.[78–81] The most popular method of incorporating electron correlation into

shielding calculations has been DFT, since it not only covers the electron correlation effect, but also is cost efficient.[82] The hybrid functional of Becke[83] and Lee, Yang and Parr,[84] known as B3LYP, continues to be among the most popular functionals of DFT calculations of chemical shielding.[82,85,86] However, some recent researches[81,87] showed that several new exchange–correlation functionals of DFT, such as KT3,[88] OPBE,[89,90] and OPW91,[89,91] perform better than B3LYP in calculation of chemical shielding. However, it should be noted that these findings apply for absolute chemical shieldings with the exception of H nucleus. To validate the performance of B3LYP with respect to KT3, OPBE and OPW91 functionals in predicting ^{1}H chemical shift for the system under studied here, we tested the four methods for isolated formamide monomer in gas-phase, using 6-311++G(d,p) basis sets. The results are listed in Table 4. As can be found from Table 4, ^{1}H NMR properties, either the absolute shielding or the relative shift, are very similar for the four functionals. The observation suggests that the hydrogen shielding or shift are quite unaffected by different xc-functionals, as observed for many other molecules as well.[79,87,92] Therefore, the B3LYP functional was still chosen for the NMR calculations in the study. However, we also note that significant differences in absolute shielding constants of carbon and oxygen nucleus are evident between B3LYP and the three new xc-funtionals, similar to some previous researches[81,87,93] on absolute shielding constants with respect to C, N, F and O nuclei. Thus, caution should be taken when the absolute shielding constant of the nuclei (with the exception of the H nucleus) is calculated using the B3LYP functional.

In addition, we, herein, present a basis set analysis for the ^{1}H shielding constant and chemical shift for isolated formamide the in gas-phase. We evaluate two basis set families recommended by previous researches,[87,93–95] *viz*. Pople-type and correlation-consistent basis sets, including 6-311++G(d,p), 6-311++G(2d,2p), aug-cc-pVTZ, aug-cc-pVQZ, aug-cc-pV5Z (see Table 5). Data in Table 5 clearly show that improvement of the basis set leads to a decrease in the absolute shielding constants and an increase in the chemical shifts. However, the differences caused by these basis sets are small for the ^{1}H chemical shifts and shielding constants. Furthermore, the ^{1}H chemical shifts calculated with the five types of basis sets display similar dependence on the dielectric constants of solvents (ε). Considering the fact that the NMR isotropic shielding constants are well converged using the aug-cc-pVTZ basis set, only the results calculated at the B3LYP/aug-cc-pVTZ level are presented in the following discussion.

Table 5 ^{1}H NMR isotropic shielding constants and chemical shifts[a] (in parentheses) of isolated formamide in the gas phase (B3LYP/6-311++G(d,p) optimized geometry) calculated using B3LYP and various basis sets[b]

Basis set	H2	H4	H9
6-311++G(d,p)	27.36 (4.61)	23.60 (8.37)	27.50 (4.61)
6-311++G(2d,2p)	26.97 (4.74)	23.22 (8.49)	23.04 (4.74)
aug-cc-pVTZ	26.85 (4.79)	23.11 (8.53)	26.83 (4.79)
aug-cc-pVQZ	26.75 (4.84)	23.06 (8.53)	26.72 (4.84)
aug-cc-pV5Z	26.70	23.03	26.66

[a] Chemical shifts of hydrogen nuclei are referred to TMS. Because TMS is too large for the NMR calculation using aug-cc-pV5z basis set, the chemical shift calculated at the B3LYP/aug-cc-pV5Z level can not be obtained. [b] Results are in units of ppm.

3.4.2 Analysis of ^{1}H chemical shifts. The calculated (GIAO B3LYP/aug-cc-pVTZ) ^{1}H chemical shifts of formamide for its isolated form and the complexed form in the gas phase and in the six solvents within the framework of the IEF-PCM model are listed in Table S2 in ESI.† Fig. 6 and 7 show predicted dependences of the variations in ^{1}H chemical shifts caused by the solvation and complexation on the solvent dielectric constants, respectively. The calculated chemical shifts of the formyl proton (δ_{H4}), either for the monomer or the complex, changes very little on going from gas phase to the different-polarity solutions. The δ_{H4} variations induced by solvents, denoted as $\Delta\delta_{H4}$(sol − gas) = δ_{H4}(in a given solution) − δ_{H4}(in gas phase), ranges from 0.02 to 0.09 ppm, nearly insensitive to the solvent polarity, as illustrated in Fig. 6. NMR experimental results of formamide reported that the δ_{H4} values are 8.12 for the gas-phase,[18] 8.15 in tetrachloroethane (TClE-d_2) solvent,[16] 7.99 in DMSO-d_6 solvent,[16] 7.85 for water-d_2 solvent[16] and 7.96 for neat solution (*viz*. formamide solvent),[16] as illustrated in Fig. 8. A similar observation from dimethylformamide determination[77] also shows that chemical shifts of the formyl proton are 8.02 for $CDCl_3$ solvent and 7.95 for $(CD_3)_2SO$ solvent and 7.92 for D_2O solvent. Similar to our results, these experimental observations also reflect the insensitivity of the chemical shift of the formyl proton to the solvent polarity. In contrast, the result calculated shows that the solvent plays significant role in the chemical shifts of amino protons, increasing their chemical shifts both in the monomer and the complex. One exception is the chemical shift of the H2 nucleus associated with the H-bonding in the complex, which is decreased as the solvent polarity increases. Significant variation in the δ_H values of amino protons due to solvation are found on going from the gas phase to CCl_4 solvent and from CCl_4 to THF, but no clear

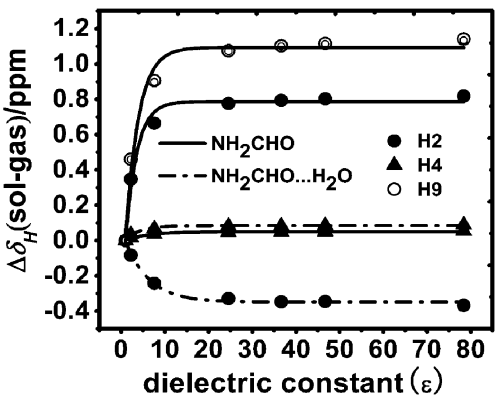

Fig. 6 Dependences of solvent-induced changes in ^{1}H chemical shifts of formamide (*viz*. $\Delta\delta_H$(sol − gas) = δ_H(in a given solution) − δ_H(in gas phase)) on dielectric constants of solvents (ε) in the monomer form (—) and the complex (---), derived from GIAO B3LYP/aug-cc-pVTZ calculation (B3LYP/6-311++G(d,p) optimized geometry). It is noted that two curves, reflecting variation trends of the $\Delta\delta_{H9}$(sol − gas) in the isolated form and the complexed state overlap, since their values in the two forms are very similar.

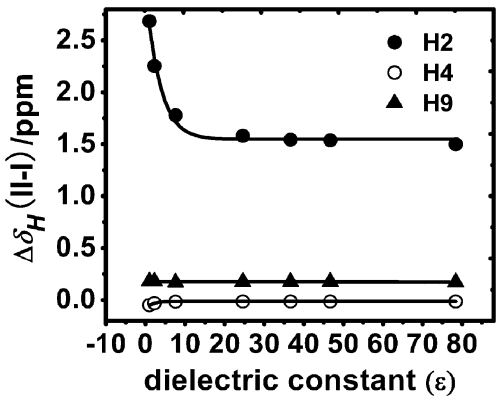

Fig. 7 Dependences of variations in ^{1}H chemical shifts of formamide upon complexation (*viz.* $\Delta\delta_H$(**II** − **I**) = δ_H (in complex) − δ_H (in monomer)) on dielectric constants of solvents (ε), derived from GIAO B3LYP/aug-cc-pVTZ calculation (B3LYP/6-311++G(d,p) optimized geometry).

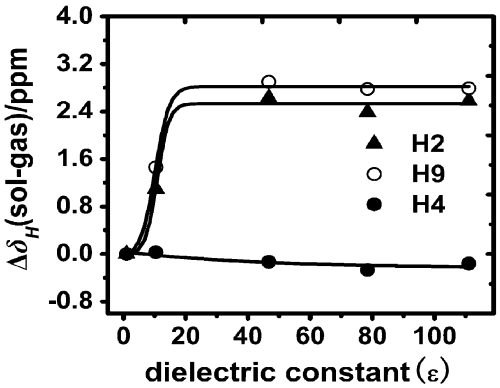

Fig. 8 Dependences of solvent-induced variations in ^{1}H chemical shifts ($\Delta\delta_H$(sol − gas)) of formamide on dielectric constants of solvents (ε), derived from experimental observations in the gas phase,[18] tetrachloroethane (ε = 10.36),[16] dimethyl sulfoxide (ε = 46.7),[16] water (ε = 78.39)[16] and formamide (ε = 110)[16] solution. The neat and water solutions are referenced to internal dimethyl sulfoxide (δ = 2.5 ppm) and the tetrachloroethane and dimethyl sulfoxide solutions, to internal TMS (δ = 0.00 ppm).

variation on the δ_H of amino protons is observed as the solvent polarity further increases (see Fig. 6). The dependency of solvation shift ($\Delta\delta_H$(sol − gas)) on the dielectric constant of environment qualitatively reproduce the experimental trend[16,18] from the gas phase to tetrachloroethane (ε = 10.36), dimethyl sulfoxide (ε = 46.7), water (ε = 78.39) and formamide (ε = 110), as shown in Fig. 8. When quantitatively compared to the experimental shifts, the calculated values underestimate the solvent effect. Probable reasons for this underestimation, or at least for a part of it, are related with the PCM computation model employed here. The PCM model is limited to non-specific solute–solvent electrostatic interactions and quantum mechanics (QM) ground states, so in principle, it is difficult to quantitatively reproduce the experimental results, which on the contrary include many other different aspects, such as the specific hydrogen bonding, van der Waals effect (mainly repulsive and dispersive interactions), temperature, *etc*. However, previous investigations showed that errors caused by these effects mentioned above are systematic in nature and some error can be partly eliminated when relative shifts are considered.[80,81,96–98] This error cancellation may be one reason that the agreement between the calculation and the experiment is often seen and assumed for relative variations in molecular properties.[48,51,53] In fact, our main interest is to present and analyze the variation trend of the molecular property caused by the non-specific solvation for the prototype compound, and accordingly to provide qualitative information for enzymes in non-aqueous media. The qualitative agreement observed between the calculation and the experiment for the gas-to-solution chemical shifts can be used to cast light on the stated purpose. An accurate analysis of the quantitative agreement between the calculated and the experimental value is beyond the scope of the present paper.

On the other hand, the differences in the δ_{H4} variations owing to the H-bonding ($\Delta\delta_{H4}$(**II** − **I**)) between the gas phase and the solvents are very small, varying within 0.05 ppm (see Fig. 7 and Table S2 in ESI†), suggesting its insensitivity to the specific H-bonding between the bound water and the amino group of formamide. Compared with the monomer, H-bonding slightly increases the δ_{H9} value of the complex. However the extent of the increase (*viz.* $\Delta\delta_{H9}$(**II** − **I**)) is small and almost unchanged from the gas phase to the six solvents (around 0.18 ppm), displaying independency on the solvent polarity (see Fig. 7). As observed above, the solvent, in the complexed form, leads the chemical shift of the H2 atom to be lowered (see Table S2 (ESI†) and Fig. 6), opposite to the result in the isolated form, implying remarkable effects of the H-bonding. Not unexpectedly, the specific H-bonding upon complexation results in a larger chemical shift for the H2 nucleus in the complex than that in the monomer. The variation of δ_{H2} induced by the H-bonding ($\Delta\delta_{H2}$(**II** − **I**)) ranges from 2.68 to 1.50 ppm when going from the gas phase to the various solutions. The solvent weakens the shift caused by the H-bonding (*viz.* $\Delta\delta_{H2}$(**II** − **I**)), especially polar solvents. Similarly, in the high-ε region (ε > 10), the $\Delta\delta_{H2}$(**II** − **I**) values are insensitive to the solvent polarity. Good linear correlations between the $\Delta\delta_{H2}$(**II** − **I**) and the two H-bonding parameters associated with the H2 atom (*viz*., the H-bond distance $r_{O6\cdots H2}$ and the electron density in the BCP of the H-bond $\rho_{O6\cdots H2}$) are obtained (eqn (7) and (8)), further revealing that it is the H-bonding of O6···H2 contact that leads to an increase in the δ_{H2} of complex with respect to the monomer.

$$\Delta\delta_{H2}(\mathbf{II}-\mathbf{I}) = 19.53 - 8.22 r_{O6\cdots H2};\ R = -0.993 \quad (7)$$

$$\Delta\delta_{H2}(\mathbf{II}-\mathbf{I}) = -2.79 + 280.84 \rho_{O6\cdots H2};\ R = 0.996 \quad (8)$$

In terms of these two correlations and some observations obtained above, we can rationalize the dependence of the $\Delta\delta_{H2}$(**II** − **I**) on the solvent polarity. The solvent weakens the H-bonding of the O6···H2 contact, and the higher the solvent polarity, the greater the weakening (*viz*. the longer is $r_{O6\cdots H2}$ and smaller is $\rho_{O6\cdots H2}$). Therefore, the $\Delta\delta_{H2}$(**II** − **I**) value is decreased as the solvent polarity increases, as shown in Fig. 7. The specific H-bonding plays more of a role than the non-specific solvation in influencing the δ_{H2} value. As a result, the $\Delta\delta_{H2}$(sol − gas) value in the complex decreases

with increase of solvent polarity, opposite to the monomer (see Fig. 6).

3.5 n → π* Vertical transition energies of formamide

UV spectroscopy is often another alternative tool to aid molecular structure and gain insight into specific information about solute–solvent interactions. Therefore, the electronic spectrum of formamide has been the focus of considerable interest for many years and is well understand *in vacuo*[28–31] though in the solution phase it has been less studied experimentally due to the complex nature of solute–solvent interaction.[26] Results from experimental studies on formamide in ACN solution[26,29] and some simple amides in water and cyclohexane solutions[27,29] already showed that solvents have a profound effect on their electronic spectra. In addition, the electronic spectrum of formamide in some solutions has been addressed by some theoretical researches using some discrete and continuum solvation models,[20–25] but mainly focused on aqueous solutions. In the work, a specific H-bonding is formed between the carbonyl group of formamide and the bound water. Therefore, it is interesting and important to understand roles of the non-specific solvation and the specific H-bonding in the n → π* transition associated with the carbonyl group of formamide.

The electronic spectra of formamide and its monohydrated complex in the six solvents are calculated using the polarized continuum TDDFT model (PCM-TDDFT) at the B3LYP/6-311++G(d,p) level, based on the PCM optimized geometries. It has been demonstrated that PCM-TDDFT calculations can yield reasonable predictions on excitation energies in solution.[12,48,50,51] The nπ* transition energies calculated are listed in Table 6. Compared with the calculated value in the gas phase, the solvents lead to the nπ* state to be blue-shifted in both the monomer and its monohydrated complex. The blue shifts upon the solvation ($\Delta E_{n\rightarrow\pi^*}$(sol − gas)) are in the range of 0.04–0.13 eV for the monomer and 0.03–0.09 eV for the complex, depending on the solvent polarity. The blue shift induced by the nonpolar solvent (CCl_4) is obviously smaller than that caused by the polar solvents. Furthermore, the shift from the nonpolar solvent (CCl_4) to the low-polarity solvent (*viz*. THF) leads to a relatively significant blue-shift but no further blue-shift is seen on going from tetrahydrofuran to the other more polar solvents (such as ETH, ACN, DMSO, water), as shown in Table 6. The blue-shift of the nπ* transition upon solvation is also reported by some theoretical studies on formamide in aqueous solution.[20,21] Accurate determination of solvent effects on the nπ* transition of formamide is difficult experimentally and reliable experimental data is lacking. The experimental work of Nielsen and Schellman showed this shift in transition energies to be small and a blue-shift of approximately 0.2–0.4 eV for the nπ* transition is observed for some simple amides in aqueous solution.[27] In addition, the predicted dependency of the n → π* transition energies on the solvent polarity is in qualitative agreement with experimental observation[99] on the UV/vis spectra of 1,1′-di-*n*-octyl-4,4′-bipyridinium diiodide in three types of solvents (*viz*. dichloromethane, methanol and water). The result from the experiment shows that the solvent causes λ_{max} of the main absorption bands to be blue-shifted and the shift is more obvious in methanol and water solutions than in dichloromethane, with the λ_{max} difference between methanol and water environment not being significant, just ∼0.05 eV, and significantly smaller than that between dichloromethane and methanol solution (∼0.09 eV).

As shown in Table 6, the blue shift induced by the polar solvents ($\Delta E_{n\rightarrow\pi^*}$(sol − gas)) is smaller in the complex (0.07–0.09 eV) than that in the corresponding monomer (0.10–0.13 eV), indicating that the H-bonding between the bound water and the solute would weaken the blue shift. Compared with the monomer, the nπ* transition energy of the complex is larger, suggesting that the specific H-bonding increases the nπ* transition energy. The solvent slightly weakens the blue-shift induced by the H-bonding (see $\Delta E_{n\rightarrow\pi^*}$(**II** − **I**) values in Table 6), but not significantly. Polar solvents play a slightly more significant role than the nonpolar solvent (carbon tetrachloride) in weakening the $\Delta E_{n\rightarrow\pi^*}$(**II** − **I**) values owing to their high ability in lowering the hydrogen bond strength, as confirmed by the observations above.

Table 6 Computed TDDFT n → π* transition energies ($E_{n\rightarrow\pi^*}$, in eV) at the B3LYP/6-311++G(d,p) level in the gas phase and in the six different solutions within the framework of the IEF-PCM model for formamide in the isolated monomer (**I**) and in the complex (**II**) and variations of n → π* transition energies upon solvation ($\Delta E_{n\rightarrow\pi^*}$(sol − gas), in eV) and upon complexation ($\Delta E_{n\rightarrow\pi^*}$(**II** − **I**), in eV)[a]

Solvents	$E_{n\rightarrow\pi^*}$		$\Delta E_{n\rightarrow\pi^*}$(sol − gas)		$\Delta E_{n\rightarrow\pi^*}$(**II** − **I**)
	I	**II**	**I**	**II**	
GAS	5.61	5.76	0.00	0.00	0.15
CCl_4	5.65	5.79	0.04	0.03	0.14
THF	5.71	5.83	0.10	0.07	0.12
ETH	5.73	5.84	0.12	0.08	0.11
ACN	5.73	5.85	0.12	0.09	0.12
DMSO	5.73	5.85	0.12	0.09	0.12
WAT	5.74	5.85	0.13	0.09	0.11

[a] **I** denotes the monomer; **II** denotes the complex; $\Delta E_{n\rightarrow\pi^*}$(sol − gas) = $E_{n\rightarrow\pi^*}$(in a given solution) − $E_{n\rightarrow\pi^*}$(in gas phase); $\Delta E_{n\rightarrow\pi^*}$(**II** − **I**) = $E_{n\rightarrow\pi^*}$ (in complex) − $E_{n\rightarrow\pi^*}$ (in monomer).

4. Conclusions

In this work, we applied the IEF-PCM model to study isolated formamide and its monohydrated complex in six different solutions owing to their implication for enzymes in organic media. The roles that the non-specific solvation and the specific H-bonding associated with the bound water play in influencing geometries, vibrational frequencies, binding energies, ^{1}H chemical shifts and n → π* transition energies, are discussed for formamide. Natural bond orbital (NBO) and atoms in molecules (AIM) theories are used to analyze the nature of H-bond interactions and the origin of solvent effects. The results indicate that the structure of formamide in solvents does not deviate much from gas-phase structure. However, significant blue-shifts of vibrational frequencies are observed for the C–N and C–H bonds whereas the other bonds show red-shifts due to the non-specific solvation and the specific H-bonding. In addition, the two effects increase the ^{1}H chemical shifts of the amino protons and the n → π* transition energy, while the chemical shift of the formyl proton is nearly

unchanged. The binding strength between the solute and the bound water is weakened by the non-specific solvation, especially in polar solvents. Therefore, it can be assumed that the enzymatic activity should be relatively low in polar solvents compared to non-polar solvents, since the bound water plays an important role in activating enzymatic activity in organic media, as confirmed by some experiments.[40]

Major differences between the complex and the monomer are mainly found in the frequencies and the chemical shift of the amino proton directly involved in the H-bonding and to a smaller degree in other properties examined. With increasing of the dielectric constant of solvent, these differences diminish, for the reason that the solvent weakens the H-bonding. In addition, the H-bonding also weakens the solvent effect through the specific intermolecular interaction, implying that the residual water plays an important role in modulating the structure and activity of enzymes in organic solvent.

In summary, compared with nonpolar solvents, polar solvents have a more obvious effect on the molecular properties. Furthermore, all the variations display a large dependency on the dielectric constant up to a value of $\sim$10, after which no further changes are observed. Although our study refers to QM ground states, which may be different from the actual situation at room temperature, some systematic errors derived from the difference may be partly cancelled when the relative variations are considered. Indeed, some variation trends predicted in the work are found to be qualitatively consistent with experimental observations, thus the results from this work could offer some insight into enzyme structure and function in organic media.

Acknowledgements

This project is supported by the National Science Foundation of China (Grant No 20775052). The authors thank referees for valuable comments on this manuscript. In addition, we deeply thank Prof. Jacob Kongsted for providing us with help in the KT3 calculation using Dalton program.

References

1 S. Blanco, J. C. López, A. Lesarri and J. L. Alonso, *J. Am. Chem. Soc*., 2006, **128**, 12111–12121.
2 F. J. Lovas, R. D. Suenram, G. T. Fraser, C. W. Gillies and J. Zozom, *J. Chem. Phys*., 1988, **88**, 722–729.
3 G. T. Fraser, R. D. Suenram and F. J. Lovas, *THEOCHEM*, 1988, **189**, 165–172.
4 B. Lucas, F. Lecomte, B. Reimann, H.-D. Barth, G. Grégoire, Y. Bouteiller, J.-P. Schermann and C. Desfrancüois, *Phys. Chem. Chem. Phys*., 2004, **6**, 2600–2604.
5 A. P. Fu, D. M. Du and Z. Y. Zhou, *THEOCHEM*, 2003, **623**, 315–325.
6 R. L. T. Parreira, H. Valdés and S. E. Galembeck, *Chem. Phys*., 2006, **331**, 96–110.
7 M. A. M. Cordeiro, W. P. Santana, R. Cusinato and J. M. M. Cordeiro, *THEOCHEM*, 2006, **759**, 159–164.
8 T. Liu, H. Li, M.-B. Huang, Y. Duan and Z. X. Wang, *J. Phys. Chem. A*, 2008, **112**, 5436–5447.
9 C.-C. Wu, J. C. Jiang, I. Hahndorf, C. Chaudhuri, Y. T. Lee and H.-C. Chang, *J. Phys. Chem. A*, 2000, **104**, 9556–9565.
10 S. T. King, *J. Phys. Chem*., 1971, **75**, 405–410.
11 M. Davies and J. Evans, *C. J. Chem. Phys*., 1951, **20**, 342–343.
12 J. C. Evans, *J. Chem. Phys*., 1954, **22**, 1228–1234.
13 J. F. Hinton and R. D. Harpool, *J. Am. Chem. Soc*., 1977, **99**, 349–353.
14 S. F. Sneddon, D. J. Tobias and C. L. Brooks, *J. Mol. Biol*., 1989, **209**, 817–820.
15 Y. Kim, S. Lim and Y. Kim, *J. Phys. Chem. A*, 1999, **103**, 6632–6637.
16 A. N. Taha and N. S. True, *J. Phys. Chem. A*, 2000, **104**, 2985–2993.
17 T. D. Ferris, P. T. Lee and T. C. Farrar, *Magn. Reson. Chem*., 1997, **35**, 571–576.
18 A. N. Taha, S. M. Neugebauer Crawford and N. S. True, *J. Am. Chem. Soc*., 1998, **120**, 1934–1935.
19 A. D. Buckingham, T. Schaefer and W. G. Schneider, *J. Chem. Phys*., 1960, **32**, 1227–1233.
20 N. A. Besley, M. T. Oakley, A. J. Cowan and J. D. Hirst, *J. Am. Chem. Soc*., 2004, **126**, 13502–13511.
21 N. A. Besley and J. D. Hirst, *J. Am. Chem. Soc*., 1999, **121**, 8559–8566.
22 A. L. Sobolewski, *J. Photochem. Photobiol., A*, 1995, **89**, 89–97.
23 N. A. Besley and J. D. Hirst, *J. Phys. Chem. A*, 1998, **102**, 10791–10797.
24 W. R. Rocha, V. M. Martins, K. Coutinho and S. Canuto, *Theor. Chem. Acc*., 2002, **108**, 31–37.
25 M. Krauss and S. P. Webb, *J. Chem. Phys*., 1997, **107**, 5771–5775.
26 P. Suppan and N. Ghoneim, *Solvatochromism*, The Royal Society of Chemistry, Cambridge, UK, 1997.
27 E. B. Nielsen and J. A. Schellman, *J. Phys. Chem*., 1967, **71**, 2297–2304.
28 J. M. Gingell, N. J. Mason, H. Zhao, I. C. Walker and M. R. F. Siggel, *Chem. Phys*., 1997, **220**, 191–205.
29 H. Basch, M. B. Robin and N. A. Kuebler, *J. Chem. Phys*., 1968, **49**, 5007–5018.
30 H. D. Hunt and W. T. Simpson, *J. Am. Chem. Soc*., 1953, **75**, 4540–4543.
31 L. Serrano-Andrés and M. P. Fülscher, *J. Am. Chem. Soc*., 1996, **118**, 12190–12199.
32 M. W. Wong, K. B. Wiberg and M. J. Frischt, *J. Am. Chem. Soc*., 1992, **114**, 1645–1652.
33 S. Moisan and J. J. Dannenberg, *J. Phys. Chem. B*, 2003, **107**, 12842–12846.
34 W. C. Liang, H. R. Li, X. B. Hu and S. J. Han, *J. Phys. Chem. A*, 2004, **108**, 10219–10224.
35 J. R. Pilegro Jr, *Chem. Phys*., 2004, **306**, 273–280.
36 Y. Xiong and C. G. Zhan, *J. Phys. Chem. A*, 2006, **110**, 12644–12652.
37 B. Mennucci and C. O. da Silva, *J. Phys. Chem. B*, 2008, **112**, 6803–6813.
38 A. M. Klibanov, *Nature*, 2001, **409**, 241–246.
39 E. P. Hudson, R. K. Eppler and D. S. Clark, *Curr. Opin. Biotechnol*., 2005, **16**, 637–643.
40 (*a*) Lu Yang, Jonathan S. Dordick and Shekhar Dordick, *Biophys. J*., 2004, **87**, 812–821; (*b*) D. S. Clark, *Philos. Trans. R. Soc. London, Ser. B*, 2004, **359**, 1299–1307; (*c*) F. Secundo, G. Carrea, C. Soregarroli, D. Varinelli and R. Morrone, *Biotechnol. Bioeng*., 2001, **73**, 157–163.
41 B. Castillo, J. Méndez, W. Al-Azzam, G. Barletta and K. Griebenow, *Biotechnol. Bioeng*., 2006, **94**, 565–574.
42 T. Anthonsen and B. J. Sjurnes, Importance of water activity for enzyme catalysis in nonaqueous organic systems, in *Methods in Nonaqueous Enzymology*, ed. M. N. Gupta, Birkhauser-Verlag, Basel, Switzerland, 2000, p. 14.
43 N. M. Micaelo, V. H. Teixeira, A. M. Baptista and C. M. Soares, *Biophys. J*., 2005, **89**, 999–1008.
44 M. N. Gupta and I. Roy, *Eur. J. Biochem*., 2004, **271**, 2575–2583.
45 A. Zaks and A. M. Klibanov, *J. Biol. Chem*., 1988, **263**, 8017–8021.
46 A. L. Serdakowski and J. S. Dordick, *Trends Biotechnol*., 2007, **26**, 48–54.
47 S. Miertus and J. Tomasi, *Chem. Phys*., 1982, **65**, 239–245.
48 B. Mennucci, *J. Am. Chem. Soc*., 2002, **124**, 1506–1515.
49 R. Cammi, B. Mennucci and J. Tomasi, *J. Chem. Phys*., 1999, **110**, 7627–7638.
50 V. N. Nemykin, R. G. Hadt, R. V. Belosludov, H. Mizuseki and Y. Kawazoe, *J. Phys. Chem. A*, 2007, **111**, 12901–12913.
51 G. Scalmani, M. J. Frisch, B. Mennucci, J. Tomasi, R. Cammi and V. Barone, *J. Chem. Phys*., 2006, **124**, 094107.

52 E. G. Bakalbassis, A. T. Lithoxoidou and A. P. Vafiadis, *J. Phys. Chem. A*, 2006, **110**, 11151–11159.
53 K. Hasegawa and T. Noguchi, *Biochemistry*, 2005, **44**, 8865–8872.
54 E. Cancès, B. Mennucci and J. Tomasi, *J. Chem. Phys.*, 1997, **107**, 3032–3041.
55 B. Paizs, P. Salvador, A. G. Császár, M. Duran and S. Suhai, *J. Comput. Chem.*, 2001, **22**, 196–207.
56 R. F. W. Bader, *Atoms in Molecules A Quantum Theory*, Oxford University Press, Oxford, UK, 1990.
57 F. Biegler-König, J. Schönbohm and D. Bayles, *J. Comput. Chem.*, 2001, **22**, 545–559.
58 A. E. Reed, L. A. Curtiss and F. Weinhold, *Chem. Rev.*, 1988, **88**, 899–926.
59 R. Ditchfield, *Mol. Phys.*, 1974, **27**, 789–807.
60 K. Wolinski, J. F. Hilton and P. Pulay, *J. Am. Chem. Soc.*, 1990, **112**, 8251–8260.
61 Dalton, An *ab initio* electronic structure program, release 2.0; 2005. See http://www.kjemi.uio.no/software/dalton/dalton.html.
62 E. Runge and E. K. U. Gross, *Phys. Rev. Lett.*, 1984, **52**, 997–1000.
63 M. J. Frisch, G. W. Trucks, H. B. Schlegel, G. E. Scuseria, M. A. Robb, J. R. Cheeseman, J. A. Montgomery, Jr., T. Vreven, K. N. Kudin, J. C. Burant, J. M. Millam, S. S. Iyengar, J. Tomasi, V. Barone, B. Mennucci, M. Cossi, G. Scalmani, N. Rega, G. A. Petersson, H. Nakatsuji, M. Hada, M. Ehara, K. Toyota, R. Fukuda, J. Hasegawa, M. Ishida, T. Nakajima, Y. Honda, O. Kitao, H. Nakai, M. Klene, X. Li, J. E. Knox, H. P. Hratchian, J. B. Cross, V. Bakken, C. Adamo, J. Jaramillo, R. Gomperts, R. E. Stratmann, O. Yazyev, A. J. Austin, R. Cammi, C. Pomelli, J. Ochterski, P. Y. Ayala, K. Morokuma, G. A. Voth, P. Salvador, J. J. Dannenberg, V. G. Zakrzewski, S. Dapprich, A. D. Daniels, M. C. Strain, O. Farkas, D. K. Malick, A. D. Rabuck, K. Raghavachari, J. B. Foresman, J. V. Ortiz, Q. Cui, A. G. Baboul, S. Clifford, J. Cioslowski, B. B. Stefanov, G. Liu, A. Liashenko, P. Piskorz, I. Komaromi, R. L. Martin, D. J. Fox, T. Keith, M. A. Al-Laham, C. Y. Peng, A. Nanayakkara, M. Challacombe, P. M. W. Gill, B. G. Johnson, W. Chen, M. W. Wong, C. Gonzalez and J. A. Pople, *GAUSSIAN 03 (Revision B.03)*, Gaussian, Inc., Wallingford, CT, 2004.
64 S. C. Meng, J. Ma and Y. S. Jiang, *J. Phys. Chem. B*, 2007, **111**, 4128–4136.
65 D. Begue, S. Elissalde, E. Pere, P. Iratcabal and C. Pouchan, *J. Phys. Chem. A*, 2006, **110**, 7793–7800.
66 U. Koch and P. L. A. Popelier, *J. Phys. Chem.*, 1995, **99**, 9747–9754.
67 P. L. A. Popelier, *J. Phys. Chem. A*, 1998, **102**, 1873–1878.
68 P. L. A. Popelier, *Atoms in Molecules: An Introduction*, Pearson Education, Harlow, UK, 1999.
69 (*a*) I. Rozas, I. Alkorta and J. Elguero, *J. Phys. Chem. B*, 2004, **108**, 3335–3341; (*b*) I. Rozas, *Phys. Chem. Chem. Phys.*, 2007, **9**, 2782–2790.
70 M. H. Cheng, X. M. Pu, N. B. Wong, M. L. Li and A. M. Tian, *New J. Chem.*, 2008, **32**, 1060–1070.
71 L. S. Gorman and J. S. Dordick, *Biotechnol. Bioeng.*, 1992, **39**, 392–397.
72 J. Meiler and D. Baker, *Proc. Natl. Acad. Sci. U. S. A.*, 2003, **100**, 15404–15409.
73 J. Meiler, *J. Biomol. NMR*, 2003, **26**, 25–37.
74 Y. Wang, *J. Biomol. NMR*, 2004, **30**, 233–244.
75 L. L. Parker, A. R. Houk and J. H. Jensen, *J. Am. Chem. Soc.*, 2006, **128**, 9863–9872.
76 A. Bagno, F. Rastrelli and G. Saielli, *J. Org. Chem.*, 2007, **72**, 7373–7381.
77 H. E. Gottlieb, V. Kotlyar and A. Nudelman, *J. Org. Chem.*, 1997, **62**, 7512–7515.
78 J. Gauss and J. F. Stanton, *J. Chem. Phys.*, 1995, **103**, 3561–3578.
79 T. Helgaker, M. Jaszunski and K. Ruud, *Chem. Rev.*, 1999, **99**, 293–352.
80 A. A. Auera and J. Gaussb, *J. Chem. Phys.*, 2003, **118**, 10407–10417.
81 A. A. Wu, Y. Zhang, X. Xu and Y. J. Yan, *J. Comput. Chem.*, 2007, **28**, 2431–2442.
82 L. B. Casabianca and A. C. de Diosa, *J. Chem. Phys.*, 2008, **128**, 052201.
83 A. D. Becke, *J. Chem. Phys.*, 1993, **98**, 5648–5652.
84 C. Lee, W. Yang and R. G. Parr, *Phys. Rev. B*, 1988, **37**, 785–789.
85 L. L. Parker, A. R. Houk and J. H. Jensen, *J. Am. Chem. Soc.*, 2006, **128**, 9863–9872.
86 T. Tuttle, E. Kraka, A. A. Wu and D. Cremer, *J. Am. Chem. Soc.*, 2004, **126**, 5093–5107.
87 J. Kongsted, *J. Chem. Theory Comput.*, 2008, **4**, 267–277.
88 T. W. Keal and D. J. Tozer, *J. Chem. Phys.*, 2004, **121**, 5654–5660.
89 N. C. Handy and A. J. Cohen, *Mol. Phys.*, 2001, **99**, 403–412.
90 J. P. Perdew, K. Burke and M. Ernzerhof, *Phys. Rev. Lett.*, 1996, **77**, 3865–3868.
91 J. P. Perdew and Y. Wang, *Phys. Rev. B*, 1992, **45**, 13244–13249.
92 D. B. Chesnut, *Chem. Phys.*, 1997, **214**, 73–79.
93 K. Aidas, A. Møgelhøj, H. Kjær, C. B. Nielsen, K. V. Mikkelsen, K. Ruud, O. Christiansen and J. Kongsted, *J. Phys. Chem. A*, 2007, **111**, 4199–4210.
94 J. R. Cheeseman, G. W. Trucks, T. A. Keith and M. J. Frisch, *J. Chem. Phys.*, 1996, **104**, 5497–5509.
95 J. N. Woodford and G. S. Harbison, *J. Chem. Theory Comput.*, 2006, **2**, 1464–1475.
96 A. K. Jameson and C. J. Jameson, *Chem. Phys. Lett.*, 1987, **134**, 461–466.
97 P. Antuono, E. Botek, B. Champagne, J. Wieme, M. F. Reyniers, G. B. Marin, P. J. Adriaensens and J. M. Gelan, *J. Phys. Chem. B*, 2008, **112**, 14804–14818.
98 P. d'Antuono, E. Botek and B. Champagnea, *J. Chem. Phys.*, 2006, **125**, 144309.
99 G. Saielli, *J. Phys. Chem. A*, 2008, **112**, 7987–7995.